

## PROPAGATION OF SPARK INITIATED LAMINAR METHANE-AIR SPHERICAL FLAMES AT CONSTANT PRESSURE

E. M. J. Mushi

Department of Mechanical Engineering, University of Dar es salaam  
P. O. Box 35131 Dar es salaam, Tanzania.

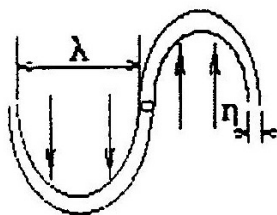
### ABSTRACT

*Spark initiated spherical methane air flames have been investigated under different discharge durations and for different equivalence ratios. Discharge duration is observed to have considerable influence on the growth of the flame which exists to very late stages of development. Discharge durations of 0.1 and 0.9 ms were observed to enhance considerably the propagation of the flame (the best being 0.9ms) compared to 0.3 and 0.7ms. The history of the flames indicate three stages of development, the first being of falling rate followed by one of increasing rate of propagation while the last is of constant rate.*

*Minimum propagation rates were observed to occur at a flame radius of between 2.5 and 4.5 mm. This radius of minimum rate of propagation is observed to increase linearly with equivalence ratio. Different rates of increase were observed for equivalence ratios below 1.0 and above. In addition there is an influence of discharge duration.*

### INTRODUCTION

The importance of laminar flames cannot be over emphasised. Understanding their behaviour facilitates understanding of the more complicated turbulent flames. Tennekes [1] suggested that the small scale



structure of turbulence may be modelled as vortex tubes of diameter of the order of the Kolmogorov scale,  $\eta$ , which are stretched by large eddies of the order of the Taylor microscale,  $\lambda$ , (Fig. 1). This led to the laminar flamelet model of premixed turbulent combustion which was observed to provide a

lead to new physical insight [2]. In this, the

premixed turbulent flame is described as an ensemble of laminar flamelets. This follows from the observation that chemical reactions in the highly dissipative vortex tubes are very fast to the extent of being instant while a finite rate does exist for the large less dissipative eddies. Chemical reactions in these large eddies tend to be laminar in nature. This implies that parameters which have an influence on the propagation of laminar flames are likely to have a similar influence on turbulent flames. Among such parameters are spark discharge duration and equivalence ratio. The current work concentrates on assessing the influence of spark discharge duration on propagation of laminar flames. This is with a main objective of enhancing the understanding of propagation of spark ignited laminar flames.

### APPARATUS AND TECHNIQUES

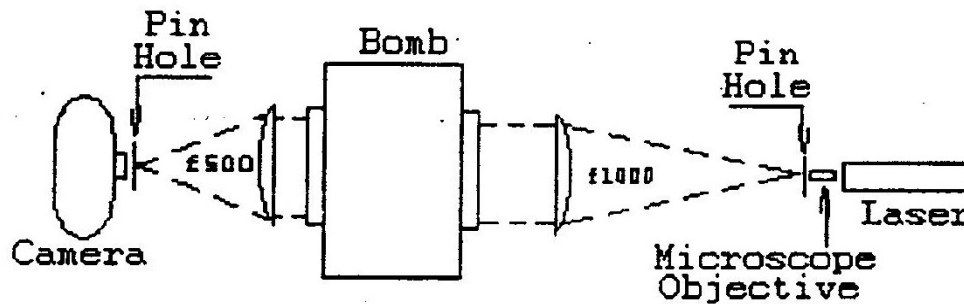


Fig.2 Schlieren Layout

Figure 2 gives the schlieren photography set-up used to record the size of the spherical flames developing from the centre of a cylindrical vessel, bomb, with a diameter of 305 mm and length of 300 mm. The vessel had 150 mm diameter concentric glass windows on each end plate for optical access.

A Spectra-Physics 10 mW helium-neon laser, model 106-1, with a beam diameter of 0.65 mm and wavelength of 632.8 nm was used. Its beam was expanded using an Olympus A40 microscope objective through a 1mm diameter pin hole. The pin hole was placed close to the objective and at the focal point of a 150 mm diameter lens. This arrangement produced a 150mm diameter beam which passed through the bomb windows. From the bomb this parallel beam was focused on to a 0.65 mm diameter pin hole using a 150 mm diameter lens with a focal length of 500 mm. Behind this pin hole was a Hitachi high speed movie camera, model 16HM, with a 35 mm lens and run at 4000 frames per second. This recorded the schlieren images of

---

---

the flame on an Ilford FP4 16 mm high speed film. The arrangement was such that on attaining the required framing speed the camera triggered an ignition unit which in turn fired a spark to ignite the mixture in the bomb. This ensured that the development of the flame was captured and at the required speed.

The developed films were projected one frame at a time on a Panasonic Telecine adapter, model WV-J20AE, which was coupled to a Panasonic CCD camera using a wide angle 28 mm lens. A Nec PowerMate 386/20 pc read the image from the camera and displayed the same on its screen from where the outer edge was traced manually using a mouse. The area enclosed by this outer edge was evaluated using numerical integration and the radius of a circle having the same area evaluated. Images of two metal markers placed on the bomb window 60 mm apart were used to convert the radius in screen units to actual size of the flame in the bomb. This resulting radius was considered to be the flame radius at that particular time. Repeating this procedure for all the frames produced flame radius-time data which after numerical differentiation gave the flame speed.

A composite spark unit was developed and used in the experiments. It consisted of three main units involving breakdown, spark and timing. Shown in Fig. 3 is a circuit diagram of the unit, without the timing unit.

The breakdown unit, which is shown to the right of the spark gap on Fig. 3, functioned as follows. On receiving a trigger pulse it energised the primary coil (PRI) of an ordinary car ignition coil with a 300 V pulse of 1 micro second duration. The secondary coil (SEC) was connected to the spark plugs via a 0.4 MegaOhms, high voltage, resistor and a high voltage diode which was only forward biased when the secondary coil voltage was high. This diode was to prevent the coil being energised by the main spark unit after the breakdown phase. The 300 V, 1  $\mu$ s pulse on the primary coil was enough to create the necessary voltage on the secondary coil to facilitate breakdown of the spark gap. The breakdown was tested both on air and on methane-air mixtures at atmospheric pressure. For both conditions the unit was found to function reliably with a maximum spark gap of 0.6mm. For larger gaps the probability of breakdown decreased sharply with increase in the gap. It was also found that for a spark gap of 0.6 mm methane-air mixtures of equivalence ratios between 0.8 and 1.25 could not be ignited using the breakdown.

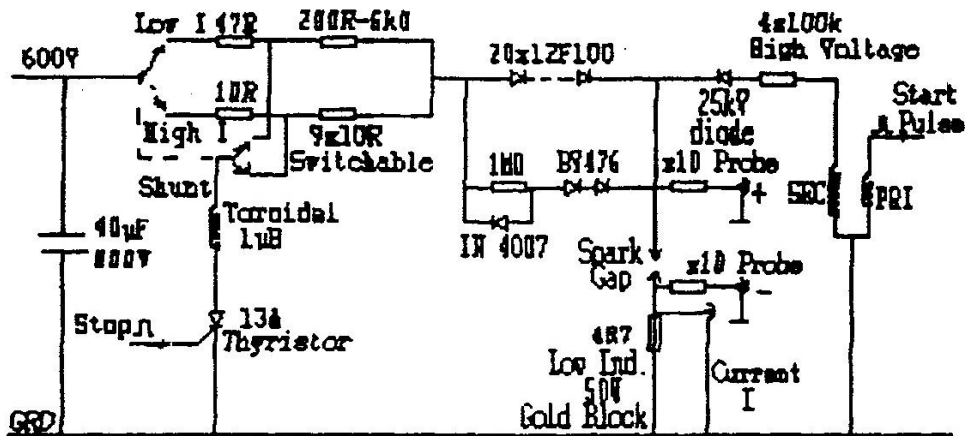


**Fig. 3 Ignition Unit Circuit**

The main spark unit was designed to discharge a 40  $\mu\text{F}$  capacitor through the spark gap via a bank of resistors which control the current. This capacitor was charged by a 600 V d.c supply. Parallel with the capacitor is a forward biased thyristor, in series with an inductor connected between the capacitor and the bank of resistors. This thyristor is triggered by the timing unit to discharge the capacitor through the toroidal inductor and hence stop the spark at the preset spark duration. The principle of operation is that when the capacitor is charging or discharging through the spark gap the gate of the thyristor is at zero voltage. When the preset spark duration is attained the timing unit sends a positive voltage pulse to the gate thus making the thyristor conductive. Under this condition, the path via the spark gap is of very high resistance compared to the one via the thyristor. It follows that the current from the capacitor is switched from the spark gap to the thyristor, thus ending the discharge. The series inductor is included to ensure safe discharge under different conditions.

Spark current control was achieved using series resistors which could be isolated or included into the circuit through switches. Increasing the series resistance of the circuit reduced the current through the spark gap, while reducing increases the current. Steps of 0.1 A and 0.75 A were used for low (0 to 3 A) and high (6 to 12 A) gap currents, respectively.

The timing unit received a start pulse generated from a control box which, in turn was triggered by the camera when it had attained the preset framing speed. On receiving this it sent the start pulse to the primary coil of the

ignition coil which initiated the breakdown phase of the spark and started counting the elapsed discharge time. When the preset discharge time was attained, the unit sent a positive pulse to the gate of the thyristor, thus ending the discharge. The time between the start and stop pulse could be varied from 0 to 1 ms in steps of 10 ms.

Two identical electrodes were mounted opposite to each other in the cylindrical walls of the combustion vessel such that they could meet at the centre, where a spark gap of 0.6mm was maintained.

Partial pressures were measured to control the composition of the combustible mixture. Prior to preparation of the mixture, the vessel was evacuated to 25 mm of mercury. Methane of 99% purity was the fuel used throughout this work. It was supplied to the vessel from a cylinder to the appropriate partial pressure. Filling of the vessel to atmospheric pressure was completed with air from a compressor. An electric heater in the vessel was used to heat the mixture while being stirred by a fan running at a low speed to ensure uniform temperature. A thermocouple inside the vessel monitored the mixture temperature. The pressure inside the vessel was measured by a mercury manometer which was also used for the measurement of partial pressures during mixture preparation. All explosions were at an initial mixture temperature of 328 K and a pressure of one atmosphere. Measurements were taken during the pre-pressure period.

After each explosion, the vessel was evacuated and flushed with air twice before further mixture preparation was done.

## **RESULTS AND DISCUSSION**

Figure 4 presents the variation of flame speed with time for different spark discharge durations. Initially, all flames indicate very high speed which decreases with time to a minimum value often close to zero. This minimum speed occurs between 0.5 and 2.3 ms after onset of ignition. This may be considered as a period of decreasing propagation rate, which is followed by a period of increasing rate where the flame speed is observed to increase with time. This in turn is followed by a period of almost constant rate where the flame speed remains relatively constant, i.e. the flame speed becomes independent of time.

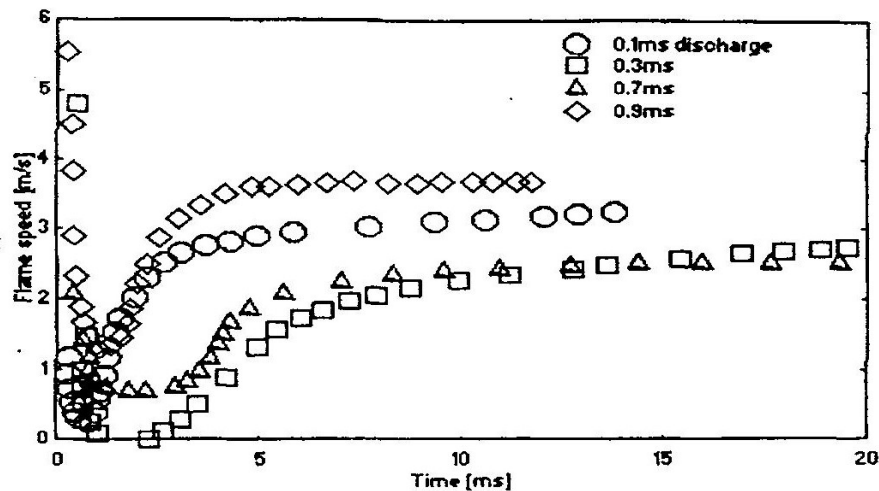


**Fig. 4 Flame speed vs time**

A spark discharge has three main modes. The first and a necessary one is the breakdown mode in which an overexponential increase in discharge current (to values of some hundreds or thousands of amperes) is observed, Maly [4]. This mode is associated with high degree of ionization and electronic excitation with massive increase in temperature. In addition, it creates a shock wave which propagates outward from the central channel. This behaviour of the breakdown mode is the reason for the initial high speed observed. Usually this mode of discharge is short lived ( a few nanoseconds ).

Depending on the ignition system the breakdown is followed by an arc and then a glow discharge or either of the two. The arc discharge is characterised by currents in excess of 100 mA and voltages of the order of 50 V. The glow discharge on the other hand is associated with low currents of order less than 100 mA. In this work the unit used had only an arc discharge after the breakdown.

Figure 5 shows the decrease in discharge power with time, for a current almost constant at 7.5 A, a discharge duration of 0.86 ms and a total discharge energy of 500 mJ. The gap voltage decrease with discharge duration implying that the arc mode tends toward a glow discharge. Maly (4) argues that energy loss through electrode conduction and radiation is up to 50% and 70% for an arc and glow discharge respectively. The decrease in gap voltage accompanied by the associated loses tend to account for the decrease in flame speed observed in the early stages. As time increases,

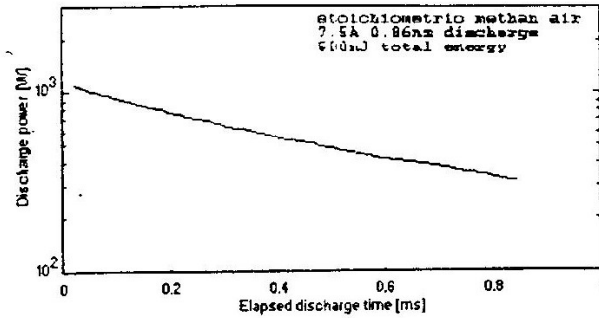


Fig. 5 Spark discharge power

less energy is available from the spark to augment the propagation of the flame. At the same time the already initiated chemical reactions have not attained rates which can generate enough heat to supplement the decrease on the spark energy.

The radius at minimum flame speed and hence the minimum propagation rate was investigated at different equivalence ratios and for two discharge durations. The results which are presented on figure 6 show considerable influence of discharge duration on this radius.

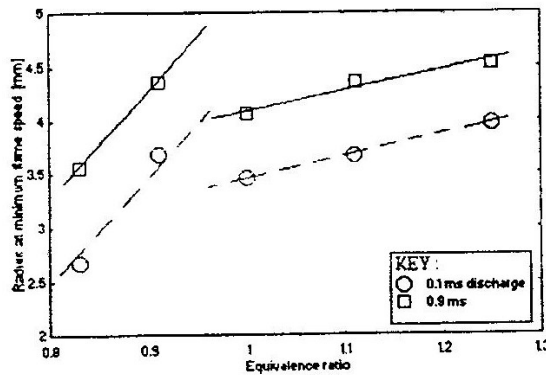


Fig. 6 Radius at minimum propagation vs equivalence ratio

Prolonged discharge gives a larger flame at the minimum propagation rate. For all the mixtures the flame radius at minimum flame speed increases linearly with equivalence ratio but between equivalence ratio of 0.9 and 1.0 there is a transition which may be a discontinuity or a transition region. The nature and behaviour of the transition could not be resolved using this work. The rate of change of the radius is higher for mixtures below equivalence ratio of 1.0, which indicates a difference in propagation rate

associated with the equivalence ratio.

Linear relationship between the radius at minimum flame speed and equivalence ratio,  $\theta$ , is obvious for  $1.0 \leq \theta$  with same rate of change of radius with  $\theta$  for the two discharge durations. For  $\theta < 1.0$  the relationship is not so obvious since only two equivalence ratios were investigated. The fitted linear curves were obtained considering that the rate of change of radius with equivalence ratio will have the same magnitude for the two discharge durations thus assuming similar behaviour to that at  $\theta \geq 1.0$ .

Since the observed variations are linear they can be represented by an equation of the form  $R_{\min} = a\theta + b$  where  $a$  and  $b$  are constants. The value of the constant  $a$  is 1.956 for  $1.0 \leq \theta$  and 10.282 for  $\theta < 1.0$ . On the other hand, the value of  $b$  varies with equivalence ratio and also it embodies some influence of the discharge. For  $\theta < 1.0$   $b$  has a value of -5.7489 for 0.1ms discharge and -4.9754 for a 0.9ms discharge. Similarly, the values for  $\theta \geq 1.0$  are 2.2433 and 1.4148 respectively.

While the rate of propagation is decreasing towards a minimum exothermic reactions are initiated within the region affected by the discharge. Though these reactions are exothermic, they require heat to sustain them. This implies that the ratio of the heat lost to that retained in the reaction zone determines the rate of these reactions. During the early stages, heat loss from the flame is through radiation, conduction via electrodes and unburned mixture and convection as a result of electrically induced turbulence, Haley and Smy [5]. When the flame is small the ratio of heat lost to that generated is very high hence the rate of the exothermic reactions is rather low. In extreme cases the heat lost may be equal to that generated and at this juncture the heat generating reactions will cease and as a result the flame will be quenched. This quenching is likely to occur at the radius where the propagation rate (flame speed) is minimum. As the flame grows the rate of heat generation increases more rapidly than the rate of heat loss. This implies that the rates of the exothermic reactions increase with the size of the flame. In addition it explains the observed increase in flame speed after the minimum value.

As the flame develops, the ratio of the heat loss to that generated decreases. In addition the influence of the burnt gases engulfed by the spherical flame



on its propagation also decreases. At a certain radius the flame loses its spherical behaviour and its characteristics resemble those of a plane flame. Under these conditions the rate of propagation remains constant.

Figure 4 does indicate a significant influence of the discharge duration on the flame speed and the manner in which it develops with time. Before minimum flame speed is attained the behaviour does not vary with discharge duration. Following the attainment of minimum flame speed differences start to emerge. Flames initiated using 0.1 and 0.9 ms discharge sparks indicate faster rate of increase of flame speed with time compared to those initiated from 0.3 and 0.7 ms sparks. In addition, the former attain constant flame speed within the first five milliseconds. The later show a two stage development from the point of minimum flame speed. First is a period of high rate of increase of flame speed and this is followed by one with rather slow rate of increase. Throughout the period of measurement these flames did not indicate attainment of constant flame speed. Further, these flames take a longer period at minimum flame speed.

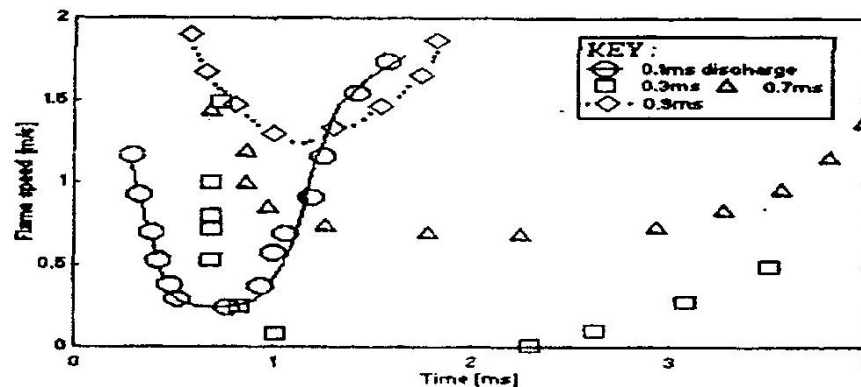


Fig. 7 Flame speed at early stages

Figure 7 gives details of flame speeds during the early stages of development. The minimum speed for 0.9ms discharge flames is 1.28 m/s which occurs at 1.16 ms after onset of ignition. This value is quite high compared to the other flames and indicates that the exothermic reactions did develop fast enough to achieve self enhancement at very early stages. Towards the end of the discharge the low power delivered together with the increased losses result in delivery of thermal energy rather than energy for massive expansion of the plasma. This in turn accelerates the exothermic reactions. On the other hand the 0.1 ms discharge flames attain a minimum flame speed of 0.21 m/s which occurs at 0.663 ms after onset of ignition.

This is followed by rapid increase in flame speed with time which is an indication of a self supporting flame. Flames from 0.3 ms discharges show a very slow recovery and their minimum speed is very close to zero.

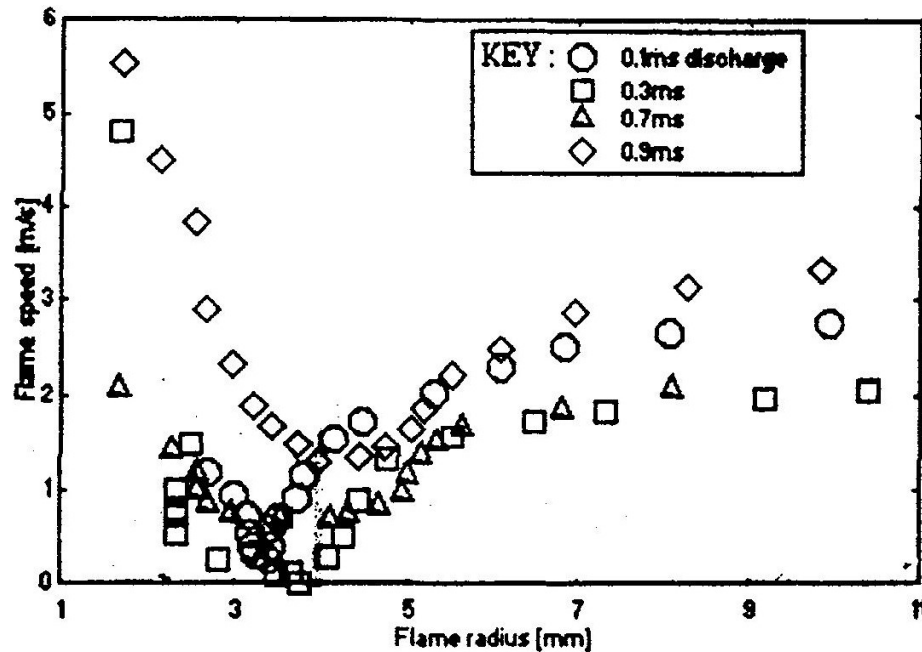


Fig. 8 Flame speed vs radius

Figure 8 presents the same information as fig. 7 but against flame radius. All flames have their minimum speed at radii between 3.4 and 4.0 mm. This indicates that on the average all the flames have minimum speed at almost the same flame radius. On the other hand figure 7 indicates a longer duration between onset of ignition and minimum speed for flames initiated by 0.3 and 0.7 ms discharges. This implies that these flames develop at a lower rate compared to the others. It is envisaged that the extra discharge energy provided in the 0.3 and 0.7 ms sparks goes into expanding ionised gases rather than providing thermal energy required to boost the exothermic reactions. Flames from 0.7 ms discharges are seen to pick up speed faster than the 0.3 ms ones. This is an indication that part of the energy for this sparks is available as thermal energy which enhances the exothermic reactions. Further investigation of Fig. 8 will show that at any given moment 0.9 ms discharges give the highest flame speed followed by 0.7 and finally 0.3 ms. Since all discharges are similar up to 0.1 ms this slow rate must be associated with the discharge after 0.1 ms.

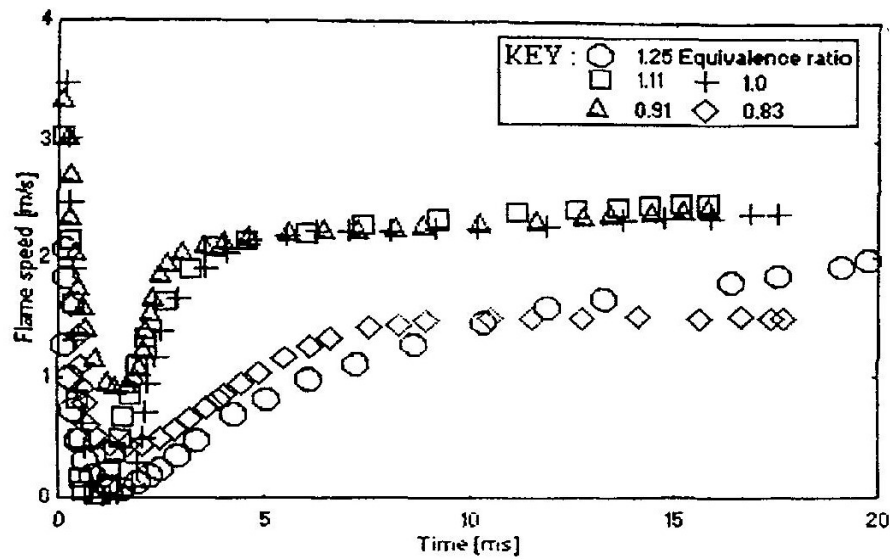


Fig. 9 Flame speed for different equivalence ratio (0.9 ms discharge)

The flame speeds for different equivalence ratio are presented on figure 9 for flames initiated using 0.9 ms discharges. Flame at equivalence ratio between 0.91 and 1.1 are observed to have a short (1.6 ms) second stage of increasing flame speed while those at 0.83 and 1.25 take considerably longer (5.7 ms). This low recovery rate may be attributed to the low heat release rate associated with such mixtures. Within each group the flame speeds are on the average of the same value at a given time. It follows from this that the influence of equivalence ratio on flame speed is not significant for equivalence ratios between 0.91 and 1.11. Similarly when it is as low as 0.83 or as high as 1.25. There is a significant difference in flame speed between the two groups.

The flame speed data can also be used to evaluate an approximate value of the laminar burning velocity,  $u_l$ . For this, the burning of entrained mixture is assumed to be adiabatic and occurs instantly. Further, the flame is assumed to be a perfect sphere. It follows from these that the mass entrained,  $dm_e$ , during a time interval  $dt$  is given by equation 1.

$$dm_e = 4\pi r_b^2 \rho_u u_l dt \quad (1)$$

$\rho_u$  is the density of the unburned mixture and  $r_b$  the radius of a sphere enclosing the combustion products. After this mass is burned, the resulting change in the total volume of the burned gas will be given by eq. 2, where  $\rho_b$  is the density of the combustion products.

$$dv = 4\pi r_b^2 (\rho_u / \rho_b) u_l dt \quad (2)$$

The rate of change of volume of a sphere of radius,  $r$ , can be evaluate as using eq. 3

$$d v = 4 \pi r^2 d r \quad (3)$$

Equations 2 and 3 yield equation 4 which on rearrangement gives an expression for the laminar burning velocity, eq. 5.

$$S = dr_b / dt = (\rho_u / \rho_b) u_l \quad (4)$$

$$u_l = S(\rho_b / \rho_u) \quad (5)$$

In the early stages of development the amount of heat lost from the reaction zone is significantly high implying that equation 5 will under estimate the burning velocity. This is because with heat loss the density of the burnt gases will be higher than that obtained under adiabatic combustion. As the flame develops the resulting error is reduced. Figure 10 shows the burning velocity evaluated for different discharge durations and presented against flame radius. Ignoring the early stages where the results have considerable error a variation in velocity associated with discharge duration is observed. The laminar burning velocity for stoichiometric methane air mixture at 328 K is 0.5 m/s, as observed by Lawes (6). This value is exceeded for the 0.9 ms discharge while the rest of the discharges give values slightly below. It is encouraging to note that the calculated values are so close to the actual burning velocity for the later stages of flame development as predicted earlier. The influence of spark discharge on the burning velocity is similar to that on the flame speed being a result of the use of constant ratio of densities.

Figure 11 gives the calculated laminar burning velocity for different equivalence ratios. Concentrating on the later stages of development it is observed that the burning velocities are very close for equivalence ratios 0.91, 1.0 and 1.11 in one group and, 1.25 and 0.83 on the other. This is in agreement with observed variation of laminar burning velocity with equivalence ratio by Andrews and Bradley [7]

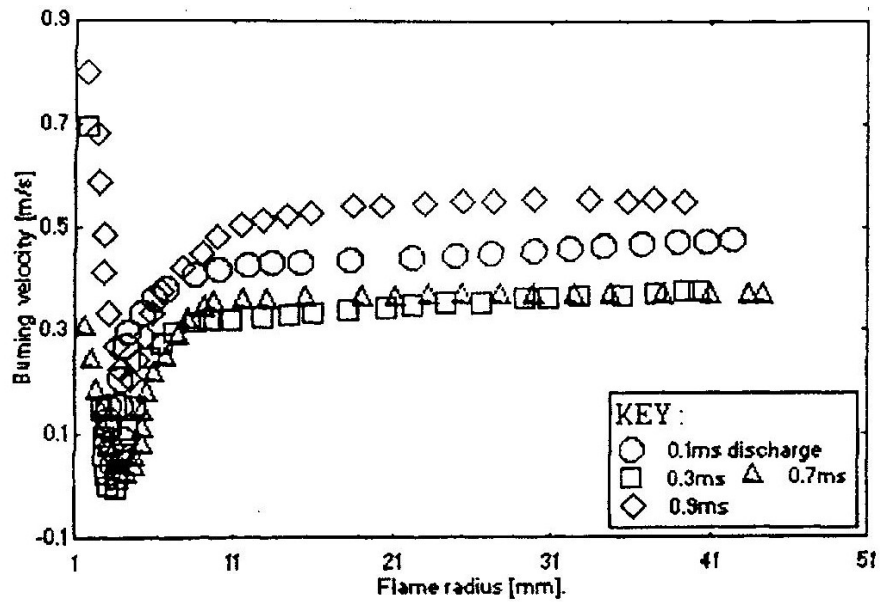


Fig. 10 Laminar burning velocity for different discharge durations

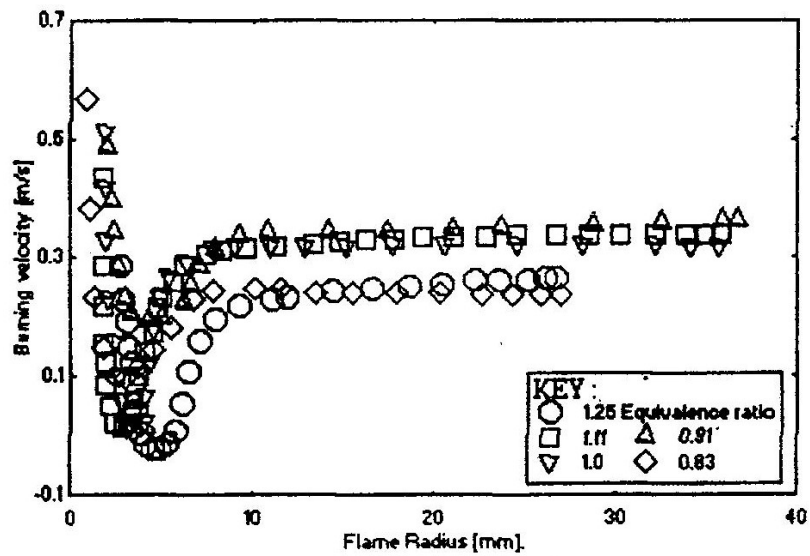


Fig.11 Laminar burning velocity for different equivalence ratio

## CONCLUSION

The development of spark initiated laminar flames occurs in three stages. The first is one of decreasing propagation rate which starts immediately on ignition. This stage is observed to be insensitive to discharge duration but the nature of the discharge is seen to influence behaviour. A second stage follows immediately after the first. This is a stage where the exothermic reactions have attained a rate by which they can sustain the flame. During this stage the propagation rate increases with time. The increase continues with diminishing returns towards the third stage where the rate of propagation is constant. At this stage, the influence of the spherical nature on the propagation of the flame does not exist hence planar behaviour can be assumed with minimum error.

Except for the first stage of propagation, there is considerable influence of discharge duration on the rates of propagation, which exhibits itself for a long period of the history of the flame. Short durations of the order of 0.1ms are seen to give improved rates compared to 0.3 and 0.7ms. On the other hand 0.9ms discharge gives the highest propagation rates. It follows that some intermediate durations may have negative effects on the flame. This implies that increased discharge duration does not always improve the thermolisation process.

Most of the flames investigated indicated minimum propagation rates at a radius between 2.5 and 4.5 mm. This seems to be a critical radius in the development of the flame. It is observed to vary linearly with equivalence ratio with different rates of change for rich and lean mixtures. In addition, this radius is also influenced by discharge duration.

## REFERENCES

1. Tennekes H., Simple model for small scale structure of turbulence  
Phys. Fluids vol. 11 no., 1968, 3 pp 669-671
2. Libby, P. A. and Bray, K. N. C, Implications of the laminar  
flamelet model in premixed turbulent combustion,  
Combustion and Flame 39, 1980, pp 33-41
3. Mushi E. J., Influence of arc discharge duration on turbulent mass

- burning rate, Uhandisi Journal vol. 18 no. 2 1994, pp 123-133
4. Maly R., Spark Ignition: Its physics and Effect on the internal combustion engine, Fuel Economy, 1984, pp 91-148
  5. Haley R. F. and Smy P. R., Electrically induced turbulence- the short duration spark, J. Phys. D: Appl. Phys. 22, 1989, pp 258-265
  6. Lawes, M., PhD Thesis University of Leeds, 1987
  7. Andrews G. E. and Bradley D., Combustion and Flame 12, 1972, pp 275-278

*The manuscript was received on 22nd October 1996 and accepted for publication, after corrections, on 29th October 1997*